Radial distribution function in x-ray-absorption fine structure

Edward A. Stern, Yanjun Ma, and Olivier Hanske-Petitpierre
Department of Physics FM-15, University of Washington, Seattle, Washington 98195

Charles E. Bouldin
National Institute of Standards and Technology, Gaithersburg, Maryland 20899
(Received 1 July 1991)

It has been argued that, in systems that have disorder too large to be described by a Gaussian, x-ray-absorption fine-structure (XAFS) spectroscopy alone cannot define the radial distribution function (RDF) because of the lack of low-k data. We show that the low-k data can, under certain conditions, be reconstructed using cumulant expansions, which give the correct functional form. This allows XAFS to determine unbiased single-shell RDF's in cases of moderate disorder, without assuming a particular model for the RDF. Some examples are given to illustrate the technique and its limitations.

I. INTRODUCTION

The extended x-ray-absorption fine-structure (EXAFS) technique has been widely used in recent years to obtain the atomic arrangement of atoms in various classes of materials whose structures are not amenable to determination by more standard techniques such as diffraction.[1,2] The fine structure past x-ray-absorption edges is produced by interference effects on the photoelectron wave function as it is backscattered by surrounding atoms.

Traditionally, it has been convenient to separate this fine structure into a region within ~30 eV of the edge, called the x-ray-absorption near-edge structure (XANES), and the region beyond, the EXAFS region.[3] The original motivation for this separation was the belief that multiple scatterings of the photoelectron wave function from the surrounding atoms was dominant in the XANES region, while single scattering was dominant in the EXAFS regions. Recent experimental[4] and theoretical[5,6] investigations have shown that multiple scatterings are not as important as first believed and by taking account of the spherical nature of the photoelectron wave function the region where single scattering is dominant extends much closer to the absorption edge. In addition, as discussed in Sec. II, only single scattering contributes to the Fourier transform isolated first coordination shell fine structure for all energies, and in some cases the same is true for the second shell. Thus, the distinction between XANES and EXAFS no longer has a justification for the fine structure when discussing the first coordination shell and in the second shell in some cases. When we are just interested in those cases we will not distinguish between XANES and EXAFS and will use the phrase *x-ray-absorption fine structure*[6] (XAFS) to describe the fine structure.

It is well known that XAFS contains the structural information of average distances to near-neighboring atoms and the types of neighbors about a specific atom type. The simple expression for XAFS also contains the mean-square variation of distances σ^2 about the average in a Debye-Waller factor of the form $\exp(-2k^2\sigma^2)$. This Debye-Waller factor is valid for small disorder or a Gaussian distribution of distances. It had also been appreciated from the very start[3] that, for more general disorder, the radial distribution function (RDF) enters into determining the EXAFS spectra. The RDF of interest is the spatial distribution of neighboring atoms relative to the specific type of center atom; that is, it is the partial pair correlation function about that type of atom.

It is usual to display the Fourier transform (and/or its magnitude) of $\chi(k)$, which is the normalized XAFS in $\mathbf{k}$ space. Here k is the wave number of the photoelectron knocked out of the atom by the absorbed photon. This Fourier transform is the convolution of the RDF and, among other factors, the backscattering t matrix of the neighboring atoms. Because of the convolution the Fourier transform is not readily related to the RDF, and further analysis has to be performed to obtain an RDF from the data. When the RDF is more complex than a simple Gaussian, there are difficulties in separating out the RDF from the XAFS. The difficulties are related to the fact that low-k information is inherently missing in the XAFS. The problems introduced by this lack of low-k information have been shown to make the determination of the RDF an ill-posed problem[7] in the sense that small errors in the XAFS and its analysis produce large errors in the RDF.

A standard method to determine the RDF is to assume a model with some variable parameters and to determine these parameters by finding the best fit between the model and the XAFS data.[1,2] If the assumed model is a poor one for the actual RDF, then large errors can ensue even though a reasonably good fit to the data can be obtained. For example, assuming a Gaussian distribution for an RDF that differs greatly from a Gaussian because it is significantly skewed about its peak will cause significant errors in the average distance and the total coordination number,[8–13] in addition to an incorrect shape to the RDF.

A good example of the problems of assuming a specific model is a disagreement over two physically distinct in-

terpretations of EXAFS data of Al-Mn quasi-crystals based on different assumed models, each of which gives a reasonable fit to the data.[14,15] This illustrates how modeling assumptions bias the results of data analysis.

Using various theoretical developments[16–19] of multiple-scattering calculations, an EXAFS data analysis program has been developed[20] that includes multiple scattering and thus can fit the full EXAFS spectrum. This then obviates the need to use a Fourier transform to isolate particular coordination shells and fits can be made to the whole spectrum at once. Although such a scheme eliminates distortions that may be introduced by Fourier filtering of particular shells, the need to include multiple scattering requires the introduction of other approximations and additional parameters whose effects have not been fully investigated and documented. Care must be exercised to limit the number of additional parameters so as not to exceed the actual amount of information present in the XAFS spectrum.[21] The approximations made, e.g., in calculating the effects of thermal vibrations on the multiple-scattering contributions, are crude and give uncertainties in the final result for the RDF that have not been fully assessed, but obviously degrade the accuracy.

In this paper we present a way to overcome the problems described above and obtain directly the RDF without biases introduced by an assumed model for the RDF. Preliminary descriptions of the method have been presented.[22] The technique at present is applicable only when one type of atom occupies the region covered by the RDF. This technique overcomes in this case one of the major criticisms of XAFS: namely, that for RDF's greatly distorted from a Gaussian, wrong answers for the RDF may be obtained if the wrong model is assumed. The analysis changes XAFS from a technique that can produce bias in the RDF by wrong assumed functional forms to one that determines the RDF with assessable errors.

II. PROBLEM

The basic expression we employ to describe the XAFS for a single shell with one type of backscatterer is[1]

$$\chi^{(k)}=\mathrm{Im}B(k)\int \exp[i2kr+\delta(k)]g(r)dr \ . \tag{1}$$

Here

$$B(k)=\frac{t(2k)}{k}\frac{m}{4\pi\hbar^2} \ , \qquad g(r)=\exp(-2r/\lambda)\frac{\rho(r)}{r^2} \ , \tag{2}$$

where Im is the imaginary part, $\rho(r)$ is the RDF defined as the probability of finding an atom in the range of radial distances from $r\rightarrow r+dr$, λ is the mean free path, and $t(2k)$ is the effective backscattering amplitude of the atoms in the shell and $\delta(k)$ the effective phase introduced by both center and backscattering atoms. Both $t(2k)$ and $\delta(k)$ have in general a weak dependence on r^{-1} because of the spherical nature of the photoelectron wave function.[6]

This expression contains certain simplifying assumptions. These are the independent particle model with single scattering and the small atom approximation. It has been shown[23] that the independent particle model is accurate to only about 20%. Multiple-scattering effects[16] could be dominant for both more distant neighbors and for near-edge structure, and the small atom or plane-wave approximation is not valid near the edge[5,6,16] where the lowest k values of the XAFS data occur.

Fortunately, by a judicious use of existing standards, these inadequacies of Eq. (1) can be canceled out.[23] The $\chi(k)$ consists of an amplitude and phase. Using a standard with the same center atom and backscattering atoms and dividing its amplitude into that of the unknown and subtracting its phase from the unknown will eliminate, to a good approximation, the errors of the independent particle approximation. If the distances in the standard are approximately the same as the unknown, then the errors of the small atom approximation are closely canceled. The multiple-scattering effects are more subtle. When one isolates the first shell by Fourier transforming, one eliminates all multiple-scattering effects.[1,16] They manifest themselves only in more distant shells at least a distance $R/2$ further than the first shell where R is the nearest-neighbor distance. In close-packed structure, such as fcc crystals, the second shell already has significant multiple-scattering contributions.[23] However, in open structures such as the diamond structure, significant multiple scatterings do not occur until past the second shell. This is a most important advantage of our method. If an isolation of the first shell were not made but one chose to fit the total XAFS spectra, the multiple scatterings of many orders could contribute near the edge and the reliability of any fit would have the added uncertainty of the accuracy of multiple-scattering calculations (which are significantly less reliable than the single-scattering calculations). The effect of any distortions introduced in isolating the first shell by Fourier transforming have been shown to be very small if properly accounted for. The advantages of eliminating multiple scatterings from consideration more than compensate for any small uncertainties introduced by Fourier transforming.

In summary, then, when good standards are used and their amplitudes are divided into and their phases are subtracted from the unknown, all of the failings of Eq. (1) are compensated for in the first shell always, and in the second shell in many cases. The resulting expression becomes

$$\exp(2k^2\sigma_s^2)\chi'(k) \ ,$$

where

$$\chi'(k)=\mathrm{Im}\int H(\Delta r)\exp(i2k\,\Delta r)d\Delta r \ . \tag{3}$$

Here

$$H(\Delta r)=\frac{\rho(r)}{r^2}\frac{R_s^2}{N_s}\exp[-2\Delta r/\lambda] \ ,$$

$\Delta r=r-R_s$, and R_s is the average distance and N_s is the coordination number of the atoms in the standard. It is assumed that the standard has small enough disorder that its distribution about R_s is given by the Debye-Waller

factor $\exp[-2k^2\sigma_s^2]$.

Because of the similarity between the standard and the unknown, λ will be closely the same in the two. Except for the λ term, this reduced $\chi'(k)$ contains only structural RDF information. Since typically $\lambda \simeq 8$ Å and $\Delta r \leq 0.5$ Å, not knowing the precise value of λ introduces only small errors.

To this point, what we have written is simply a standard XAFS analysis procedure for the first shell. The term $\chi'(k)$ is the oscillatory quantity that is due only to structure which is left once the atomic backscattering phase and amplitude terms are eliminated. In the case of small disorder, the XAFS phase and amplitude are not usually recombined into an oscillatory term, $\chi'(k)$, because the phase contains distance information while the amplitude contains the coordination number and Debye-Waller factor. In the case of small disorder it is therefore advantageous to treat phase and amplitude separately after atomic functions are removed. However, in the large disorder case, recombining the purely structural parts of the phase and amplitude into $\chi'(k)$ allows us to produce formally the desired $\rho(r)$ by the Fourier transform:

$$\rho(r)=\frac{r^2N_s}{R_s^2}\exp\left[\frac{2\Delta r}{\lambda}\right]\int_0^\infty \chi'(k)\sin(2k\,\Delta r)dk \ . \tag{4}$$

The inversion of Eq. (4) is a formal result. The main limitation on this procedure is that we do not have available the k range from $0\rightarrow\infty$. In actuality, the available k range is limited by the experiment. The upper limit k_2 is set by the backscattering amplitude decreasing at high photoelectron energy into the noise. The lower limit k_1 is set by various factors. As mentioned above, for the first shell in all cases and for the second shell in open structures, multiple scattering does not limit k_1. It is limited by the lifetime of the excited state, experimental difficulties of separating the atomic absorption from the XAFS near the edge, and the Pauli exclusion principle.

The Pauli exclusion principle sets the edge at the first unoccupied state. For a metal this occurs at a value of $k_1=k_F$, the Fermi wave number, which is typically 1–1.6 Å^{-1} For nonmetals, the relevant quantity is the energy of the edge above the muffin-tin zero, which translates to similar values of k_1. The lifetime of the excited state for a 10-keV K edge corresponds to a 3-eV broadening of energy levels, which corresponds to a $k_1 \simeq 0.9$ Å^{-1}.

The $\chi(k)$ is defined by

$$\chi(k)=\frac{\mu-\mu_0}{\mu_0} \ , \tag{5}$$

where μ is the measured absorption coefficient in the condensed state with its XAFS and μ_0 is the atomic value. Usually, μ_0 is not known experimentally, and it is assumed that it is smoothly varying. However, near the edge, the atomic μ_0 is also rapidly varying as it initially increases and possibly reaches a single maximum or several maxima (e.g., making transitions to bound atomic levels). Thus, it is not usually possible to separate μ_0 from μ very near the edge, though in the case of the K edge of Pb metal, this separation has been accomplished.[24] This separation becomes possible typically 10 or more eV past the edge where the μ_0 variation becomes smooth. Adding this energy to the Fermi energy of 5–10 eV gives a value of $k_1 \approx 2$ Å^{-1}.

The dominant factors in determining k_1 are the Pauli exclusion principle and the experimental difficulties of separating μ_0 from μ, giving a typical value of $k_1 \approx 2$ Å^{-1}. The maximum value k_2 depends on the atomic number Z of the neighboring atoms. Low-Z atoms have a backscattering amplitude that drops off rapidly at high k, so that $k_2 \simeq 10$ Å^{-1} before the noise in the XAFS starts obscuring the signal. High-Z atoms such as Pt, Ta have significant backscattering amplitudes even to values of $k_2=20$ Å^{-1} but can be attenuated to lower k_2 values by disorder.

Thus, in practice, the experimental data permit one to integrate Eq. (4) over the range $k_1\rightarrow k_2$ to obtain an approximation to $\rho(r)$ given by

$$\rho(r)\approx\frac{r^2N_s}{R_s^2}\exp\left[\frac{2\Delta r}{\lambda}\right]\int_{k_1}^{k_2}\chi'(k)\sin(2k\,\Delta r)dk \ . \tag{6}$$

The main difference between Eqs. (4) and (6) is that, in reality, we can only measure $\chi'(k)$ over a finite range in k. The high-k limit, k_2, is not a serious limitation since its main effect is to limit the spatial resolution of $\rho(r)$ to

$$\delta r \approx \frac{1}{2k_2} \ , \tag{7}$$

where the factor of 2 in Eq. (7) comes from the variable in the sine function of (6) being $2k$ instead of k. However, the lower limit k_1 causes problems. It introduces spurious variations in $\rho(r)$ that obscure its true variation. It is lack of the low-k information that has led to the belief that inversion of Eq. (6) is not possible. However, we give below a prescription to recover the low-k information so that the inversion process can be carried out.

III. SOLUTION

As shown above, it is the lack of low-k information that precludes inversion of $\chi'(k)$ to yield what we want, $\rho(r)$. To carry out the inversion indicated in Eq. (6) will always involve some type of extrapolation of $\chi'(k)$ to $k=0$ in order to "restore" the missing data at low k. However, there are constraints that rule out a large number of possible RDF's, because not all extrapolations of the data to $k=0$ are physically consistent with the data at higher k.

The physical basis for this argument is that for small enough k, all possible RDF's look Gaussian. The reason for this is that, at such low k, the width of the distribution becomes small compared to the photoelectron wave number, and the photoelectron scattering process can only sense that the distribution is, to first order, perturbed from a δ function. The first-order correction, as shown below, is a Gaussian term, which guarantees that near $k=0$, the behavior of the natural logarithm of the amplitude of $\chi'(k)$ goes as k^2. We are sufficiently near

$k=0$ when $k\sigma \ll 1$.

As k becomes larger the photoelectron wave number can begin to resolve more structure in the distribution and this increased resolution leads to corrections to the Gaussian distribution that are described by the cumulant expansion. From the definition of cumulants[1,25,26]

$$\begin{aligned}\chi'(k)&=\mathrm{Im}\int H(\Delta r)\exp(i2k\,\Delta r)d\,\Delta r\\&=\mathrm{Im}\exp\sum_{n=1}^{\infty}\frac{(2ik)^n}{n!}C_n\\&=\mathrm{Im}Q(k)\exp[i\Phi(k)]=Q(k)\sin\Phi(k)\ ,\end{aligned}\tag{8}$$

where C_n is the nth-order cumulant average. In terms of ordinary moments, the leading cumulants are

$$C_1=\langle\Delta r\rangle=R-R_s\ ,\quad C_2=\langle(r-R)\rangle^2=\sigma^2\ ,$$
$$C_3=\langle(r-R)^3\rangle\ ,\quad C_4=\langle(r-R)^4\rangle-3\sigma^4\ .$$

The average over $H(\Delta r)$ is denoted by $\langle\ \rangle$. Both $Q(k)$ and $\Phi(k)$ are real and are given by

$$\begin{aligned}Q(k)&=\exp\left[\sum_{n=0}^{\infty}(-1)^n\frac{(2k)^{2n}}{(2n)!}C_{2n}\right]\ ,\\\Phi(k)&=\sum_{n=0}^{\infty}(-1)^n\frac{(2k)^{2n+1}}{(2n+1)!}C_{2n+1}\ .\end{aligned}\tag{9}$$

Note that the natural logarithm of the amplitude of the reduced $\chi'(k)$ is even in powers of k while the phase $\Phi(k)$ is odd in powers of k.

We will next find the conditions that make such an expansion a good approximation when only the first few terms are kept. In determining the RDF by diffuse scattering of x rays or neutrons, it is possible to obtain much lower values of k_1 than is possible by XAFS, especially using small-angle scattering. The wave number used in that case is $q=2k$, and the quantity corresponding to $\chi'(k)$ typically shows large variations below $k_1=2$ Å^{-1}. These variations cannot be described by the first few terms of (9) but require the full expansion. In that case the data below k_1 cannot be reconstructed from the data above k_1. It can only be reconstructed if it is known that the data below k_1 can be accurately described by just the first few terms of Eq. (9). Then a smooth fit of such an expansion for the data above k_1 can be extrapolated below k_1 to reconstruct the data in the range.

Examples of the latter behavior occur frequently in XAFS. If an isolated shell has a disorder that can be described by a Debye-Waller factor, then only the first term in Φ and the first two terms in Q are present in the expansion and the extrapolation is easily performed. A natural logarithm plot of Q versus k^2 is a straight line[1] that is easily extrapolated to the origin while the plot of Φ versus k is also a straight line[1] that is also easily extrapolated to the origin.

The difference between the case of diffuse scattering and the XAFS example is the range of r described by $\chi'(k)$. In the XAFS case only a single shell is being considered while in the diffuse scattering case the RDF from the origin out to many angstroms is being measured. By limiting the range in **r** space to a sufficient degree, the variation in **k** space can be made as smooth as desired. A conservative estimate is[27]

$$Dr\,\delta k=\pi/2\ ,\tag{10}$$

where Dr is the range over which $\rho(r)$ varies significantly and δk is the spacing between points in **k** space where $Q(k)$ and $\Phi(k)$ can vary significantly. Thus, if

$$Dr<\pi/2k_1\ ,\tag{11}$$

both $Q(k)$ and $\Phi(k)$ vary smoothly between $0<k<k_1$ and their expansion in terms of the first few cumulants is valid.

From Eq. (11) and the value of $k_1=2$ Å^{-1}, the range of $\rho(r)$ that can be determined is

$$Dr\le 0.8\ \text{Å}\ .\tag{12}$$

In practice this limit is too conservative since it applies to the extreme case of $\rho(r)$ equal to two δ functions a distance Dr apart which cause a beat minimum to occur in $\chi'(k)$ at the k value of Dk given by Eq. (12). In the more usual case of a smoother distribution in $\rho(r)$ the behavior in $\chi'(k)$ will also be smoother, and it is possible to extend the range of Dr beyond that given by Eq. (12) to typically 1–1.2 Å. A numerical example illustrating this is given in the next section.

Using the extrapolation to $k=0$ it is now possible to calculate

$$\rho(r)\approx\frac{N_s r^2}{R_s^2}\exp\left[\frac{2\,\Delta r}{\lambda}\right]\int_0^{k_2}\chi'(k)\sin(2k\,\Delta r)dk\ ,\tag{13}$$

which is now a faithful presentation of $\rho(r)$ with a limited spatial resolution given by Eq. (7). However, using a sharp cutoff in the integral in Eq. (13) at $k=k_2$ can introduce spurious wiggles in $\rho(r)$ if the integrand has an appreciable magnitude at $k=k_2$. In that case the cutoff wiggles can be decreased by adding a Gaussian factor $\exp(-2k^2\sigma_c^2)$ such that $\exp(-2k_2^2\sigma_c^2)\ll 1$. In such a case the spatial resolution, from Rayleigh's criterion, is determined by this convergence factor, and it is given by

$$\delta r=2.5\sigma_c\ .\tag{14}$$

The important insight obtained from this discussion is that lack of low-k data does not prevent the determination of an RDF, as is sometimes claimed,[8] but simply limits the range Dr over which the RDF can be obtained at any one analysis. Within this range Dr the RDF can be accurately defined. By treating each shell separately, several coordination shells can be analyzed even when their separation is greater than the Dr of Eq. (11) as long as each shell is localized within Dr.

The three major limitations of this procedure are the following: (1) The region over which $\rho(r)$ can be determined is limited by multiple-scattering effects. Multiple scattering limits the determination of $\rho(r)$ to within $1\frac{1}{2}$ times the average of the nearest-neighbor shell distance in close-packed structures and to the first and second shells in open structures. (2) The process only works when

there is a single type of atom in the shell that is being analyzed. (3) The analysis method will fail if the spread Dr is too great, so that the cumulant expansion at k_1 requires a large number of terms. However, in a number of systems with moderate to surprisingly high disorder, this process can produce an unbiased extraction of $\rho(r)$. Examples are given below.

IV. EXAMPLES OF APPLICATION

In this section we first show an example of $\rho(r)$ determined by the method described in the previous section. This example will illustrate more clearly the problem involved and accuracy with which $\rho(r)$ can be obtained. The example we present is the first coordination shell of atoms about Mn atoms in the crystalline α phase of Mn-Al-Si, whose structure is known[28] and whose RDF about the Mn atoms is complicated enough that it does not fit a simple modeling function. The α phase also will test the requirement of having only one type of atom in the shell, because the first shell contains a small fraction of Si atoms mixed with the Al atoms. The details of the XAFS measurements are presented elsewhere.[29] The standard employed for the Mn-Al scattering is the crystalline-phase orthorhombic $MnAl_6$. The Al atoms do not have a simple Gaussian distribution about the Mn atoms in the orthorhombic phase. However, the phase has only one Mn site with a known[30] narrow distribution, whose effect can be corrected for by dividing its $\chi_s(k)$ by

$$\mathrm{Im}\sum_j \frac{\exp(ikr_j)}{r_j^2}\exp[-i2(r_j-R_s)/\lambda] .$$

Here r_j is the position of the jth Al atom and R_s is the average position of the Al atoms. After the division the resulting $\chi_s(k)$ has a simple Gaussian distribution due to vibrations, and it is used as the standard. In this case, the temperature dependence of its σ_s^2 is the same as the σ^2 of the α phase and thus the Debye-Waller factor (DWF) of the standard approximately cancels the DWF of the α phase.

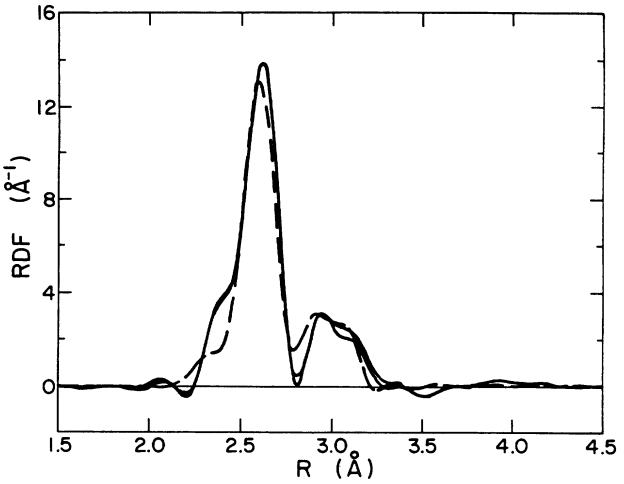

FIG. 1. Measured (solid) and calculated (dashed) radial distribution function of the nearest-neighbor atoms about Mn atoms in α-(Mn-Al-Si). In all curves the resolution is 0.063 Å. The two solid curves are independently measured, indicating experimental uncertainties.

The resulting $\rho(r)$ of Eq. (13) using a convergence factor with $\sigma_c^2=0.004$ Å^2 and $\sigma_s^2=0$ is shown in Fig. 1 by the two solid curves. Each curve is an independent determination of $\rho(r)$ using independently measured scans of the XAFS of α-(Mn-Al-Si). The variations are a measure of the uncertainties in the measured RDF. The spatial resolution is given by $\sigma_c=0.063$ Å. The r-space window employed to define the limits of $\rho(r)$ is between 1.4 and 2.7 Å in the Fourier transform of $\chi(k)$, which is displaced from the true values[1,2] by shifts introduced by $\delta(k)$. This experimental result is compared with the RDF calculated from the published structure[28] of the α phase. This calculated RDF is obtained by performing a $\sin(2kr)$ transform of

$$\chi_\alpha(k)=\frac{1}{2}\exp(-2k^2\sigma_c^2)\mathrm{Im}\sum_{m=1}^{2}\sum_j \frac{\exp(i2kr_{jm})}{r_{jm}^2}\exp[-2(r_{jm}-R_m)/\lambda] . \quad (15)$$

Equation (15) contains the same convergence factor as was used for the experimental curve. There are two Mn sites in the α phase, and r_{jm} is the position of the jth neighbor about the mth Mn site. R_m is the average distance between the mth site of Mn and its neighbors. The transform of (15) gives the calculated RDF with the same spatial resolution as was used for the experimental determination and is plotted as the dashed curve in Fig. 1.

Note several features of the results shown in Fig. 1. The negative values of the experimental RDF are very small. Nothing in the procedure inherently prohibits negative contributions, and their absence is an independent measure of how well the procedure is working and how well the nonstructural factors $t(2k)$ and $\delta(k)$ have been eliminated. This indicates that the mixture of a small number of Si atoms introduces insignificant errors. The experimentally determined RDF after eliminating $t(2k)$ and $\delta(k)$ is qualitatively similar to the calculated one. They both show a large peak around 2.5 Å, with a shoulder at the low-r part. They also both show a separated double-peaked structure centered around 3 Å.

The validity of keeping only the first few terms in the cumulant expansion [Eq. (9)] can be checked by this model. In Fig. 2 is shown the plot of the calculated amplitude and phase of $\chi_\alpha(k)$ of Eq. (15). There is a spread in distances in the first shell of α-(Mn-Al-Si) of $Dr=3.07-2.27$ Å$=0.80$ Å, as determined by diffraction. According to criterion (11), the amplitude and phase can be approximated by the first few terms of the cumulant expansion for

$$k_1 < \frac{\pi}{2\times 0.80} = 1.85 \text{ Å}^{-1} .$$

As can be noted from Fig. 2, where the first two k-dependent terms of the cumulant expansion are plotted as the dashed curves and compared with the amplitude and phase of $\chi_\alpha(k)$, this criterion is valid. In fact, it is at least a factor of 1.3 too conservative, as the expansion is valid to $k_1 \simeq 4.0$ Å^{-1} for the phase and $k_1 \simeq 2.5$ Å^{-1} for the amplitude.

The second example we present is a more critical test of the need to have a single backscatterer in the shell in order to obtain an accurate RDF. The RDF will be calculated about the Fe atoms in the metalloprotein of the azidomet form of hemerythrin, which contains a mixture of three oxygen and three nitrogen atoms. Oxygen and nitrogen differ by one atomic number and therefore have reasonably small differences in their $t(2k)$ and $\delta(k)$ but a larger difference than between Al and Si. We will compare the RDF determined by eliminating the $t(2k)$ and $\delta(k)$ using, in turn, those of oxygen and nitrogen.

The biological protein hemerythrin serves an oxygen transfer and storage function in some marine worms.[31] It serves the analogous function to hemoglobin in mammals. The active site of the azidomet form of hemerythrin contains two Fe atoms coupled by sharing a common oxygen atom as a nearest neighbor,[32] called a μ-oxo bridge. The other first-neighbor atoms are all oxygens and nitrogens. Because the first shell consists of two types of atoms, the RDF of this shell traditionally has been determined by fitting to a model containing overlapping shells of oxygen and nitrogen atoms. However, because the $t(2k)$ for oxygen and nitrogen are similar (their atomic numbers only differ by one) the modeling usually cannot distinguish between the nitrogen and oxygen atoms.

The RDF is determined using two different standards, one representing the $t(2k)$ and $\delta(k)$ for Fe-O and the other representing the $t(2k)$ and $\delta(k)$ for Fe-N. Since the first shell is a mixture of the O and N atoms, the two RDF's determined by the two standards represent two extremes.

The standard for the Fe-O backscattering is Tri-μ_3-oxo-triaquo-hexakis(glycine)triiron(III)perchlorate. Its first-neighbor shell about the Fe consists of six oxygens at an average distance of 2.02 Å with a structural mean-squared disorder of 0.0031 Å^2, which can be well approx-

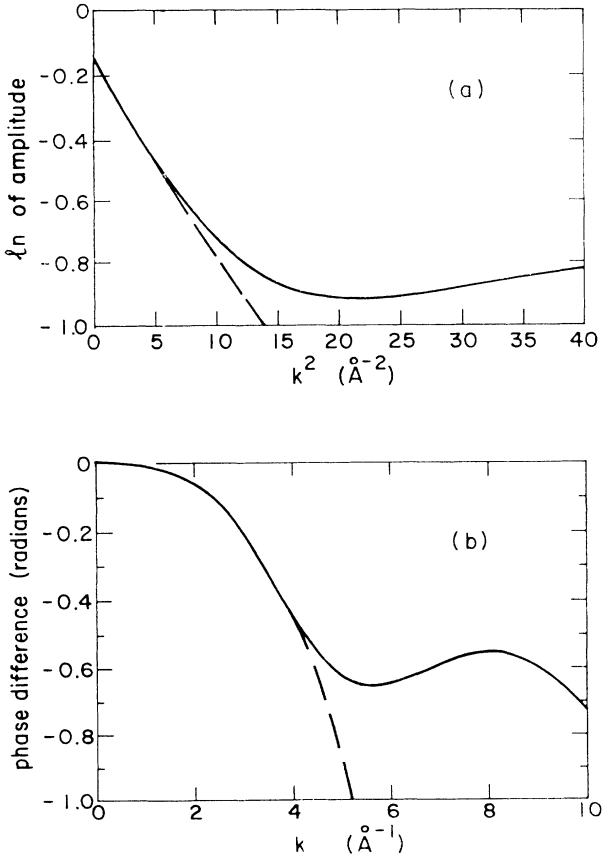

FIG. 2. (a) The natural logarithm of the amplitude and (b) the phase $\Phi(k)$ of the calculated $\chi_\alpha(k)$ of α-(Mn-Al-Si) plotted on an expanded scale vs k^2 and k, respectively (solid curves). The first two k-dependent terms in the cumulant expansion are plotted as the dashed lines for the two.

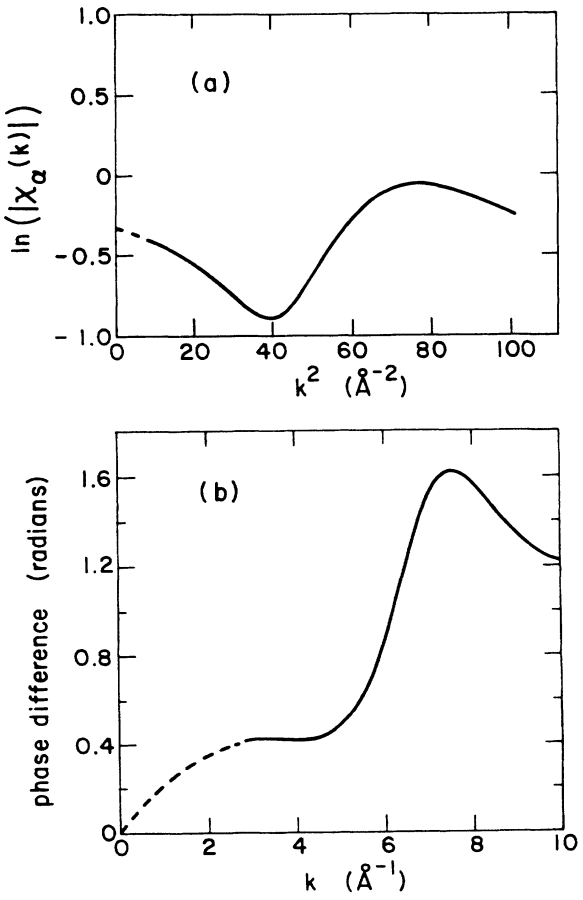

FIG. 3. (a) Natural logarithm of amplitude and (b) phase of $\chi'(k)$ for the iron site in azidomethemerythrin using a Fe-O standard. The solid curve is obtained from the measurement, and the reconstructed low-k data is shown by the dashed curve.

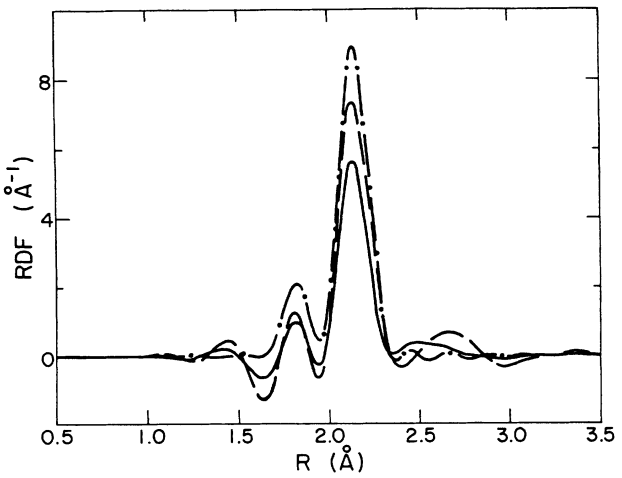

FIG. 4. The RDF's of azidomethemerythrin obtained by using a Fe-O standard (solid) and a Fe-N standard (dashed) and calculated using the results obtained by fitting a model to EXAFS data (dot-dashed). The latter is the correct RDF.

imated by a simple Gaussian. The standard for the Fe-N backscattering is bis(acetonitrile)-(2,3,9,10-tetramethyl-1,4,8,11-tetraaza-cyclotetradeca-1,3,8,10-tetranene) iron(II)hexafluorophosphate. The first-neighbor shell about the Fe consists of six nitrogens at an average distance of 1.94 Å, with a structural mean-squared disorder of 0.0001 Å^2, which is also small enough to be approximated by a simple Gaussian.

The phase and natural logarithm of the amplitude of the resulting $\chi'(k)$ using the Fe-O standard is shown in Fig. 3 with the reconstructed low-k data. Some problem already is evident because the intercept at $k=0$ for the natural logarithm of the amplitude is too low. From the known structure the predicted intercept is -0.16, while the actual one is -0.3. Figure 4 shows the RDF's obtained by using the Fe-O standard, the Fe-N standard, and the one obtained by simulating the structure determined by a fitting routine to the XAFS data.[32] Note that the two RDF's plotted in Fig. 4 using the method of this paper have large negative values, indicating that the $t(2k)$ and $\delta(k)$ factors have not been completely eliminated. It is of interest that the differences between N and O backscatterers produce such large effects which were not present in the first example. Also, note that the differences between the measured RDF's and the calculated RDF is about the same as the magnitude of the negative values, suggesting that the negative values are a good measure of the errors in the RDF.

V. DISCUSSION AND CONCLUSIONS

The procedure for calculating RDF's from XAFS data has the virtue of giving an answer without introducing biases by assuming a model for the RDF. This overcomes one of the major criticisms of XAFS, namely, that it gives wrong answers when the disorder is large. The new procedure gives an answer with assessable errors. The absence of low-k data limits the range in r space, Dr, over which the RDF $\rho(r)$ can be determined to around 1 Å. This procedure extends the type of disordered systems that can be analyzed by XAFS. If the $\rho(r)$ of a single shell is broader than 1 Å, then the EXAFS analysis misses this contribution. This is because there is not sufficient XAFS data above k_1 to allow a meaningful extrapolation of the data from $k=k_1$ to $k=0$. Therefore, this analysis method will not allow XAFS to handle as extremely disordered systems as can be handled by x-ray scattering, where much lower k data can be determined. However, we do obtain an accurate reconstruction of $\rho(r)$ in cases of moderate to reasonably high disorder.

The procedure was not invalidated by the mixture of a small fraction of Si atoms with Al, but it was invalidated by equal numbers of N and O atoms. This difference is caused by two factors. Though the atomic number difference in the atoms mixed in the shell is unity in both cases, the difference in $t(2k)$ and $\delta(k)$ is larger for the N and O pair than for the Al and Si pair because the percentage difference in atomic number is smaller in the latter case. Also, the fraction of Si is only about 10%, while equal numbers of N and O atoms are present in the second example. The procedure can always be applied to the nearest-neighbor atoms and to next-nearest-neighboring shells of atoms in open structures and perhaps to more distant atoms, but the perturbations introduced by multiple scatterings at these larger distances need to be assessed further to determine how serious are the inaccuracies they introduce.

Besides inaccuracies introduced by multiple scattering at the large distances, other inaccuracies are introduced at shorter distances by deviations from the plane-wave approximation and uncertainties in the value of the mean free path. Fortunately, the latter two effects are small. The assumption employed in the procedure is that the backscattering amplitude $B(k)$ is only weakly dependent on the distance r of the backscattering atom from the origin. Because of the breakdown of the plane-wave approximation there is a weak r dependence in $t(2k)$ and $\delta(k)$, which is approximately linear in $1/r$ within a shell, and even a good standard with the same average distance between the center atom and the backscatterer as the unknown would not completely cancel this dependence because, in general, their $\rho(r)$ are different. Fortunately, this r dependence is quite small and can generally be neglected for ranges of Dr where the cumulant expansion is effective.

Although multiple-scattering effects may be present at larger values of r, this by itself does not mean that it is not possible to obtain $\rho(r)$ by the procedure described here. It is possible by using a good standard that has similar multiple-scattering effects at similar distances that the ratio of amplitudes and differences of phases will be dominated by changes in the RDF and the analysis will give reasonably accurate results for $\rho(r)$. Further investigations are necessary to test the limitations at larger distances and to determine how to account for multiple-scattering effects if they are important.

One measure of success of the procedure is the size of the negative values of $\rho(r)$ in the examples of the previous

section. Any inconsistency or errors in the procedure would not eliminate completely the large negative values that are obtained in the standard Fourier transform of $\chi(k)$. One has, thus, an inherent check on the accuracy and correctness of the procedure by looking at the final $\rho(r)$ and noting the size of the negative regions.

When the atoms in the nearest coordination shell are an overlapping mixture of ones with quite different atomic numbers, the procedure described here does not apply. In that case modeling can be used but with the attendant possibility of adding biases that may give wrong answers. It may be possible to obtain partial RDF's for each type of atom by judiciously taking natural-logarithmic ratios of amplitudes and differences of phases separately with standards that contain only one type of the backscattering atoms. Further investigations of these cases should be pursued.

ACKNOWLEDGMENTS

We are grateful to John Rehr for introducing the cumulant expansion to us. The research was supported partially by the U.S. Department of Energy under Contract No. DE-A505-8-ER10742 and by NSF Grant No. DMR80-2222.

[1]E. A. Stern and S. M. Heald, in *Handbook of Synchrotron Radiation,* edited by E.-E. Koch (North-Holland, New York, 1983), Chap. 10.

[2]P. A. Lee, P. H. Citrin, P. Eisenberger, and B. M. Kincaid, Rev. Mod. Phys. **53**, 769 (1981).

[3]E. A. Stern, Phys. Rev. B **10**, 3027 (1974).

[4]G. Bunker and E. A. Stern, Phys. Rev. Lett. **52**, 1990 (1984); **54**, 2726 (1985); D. D. Vvedensky and J. B. Pendry, *ibid.* **54**, 2725 (1985); C. E. Bouldin, G. B. Bunker, D. A. McKeown, R. A. Forman, and J. J. Ritter, Phys. Rev. B **38**, 10816 (1988).

[5]J. E. Müller and W. L. Schaich, Phys. Rev. B **27**, 6489 (1983); W. L. Schaich, *ibid.* **29**, 6513 (1984).

[6]J. J. Rehr, R. C. Albers, C. R. Natoli, and E. A. Stern, Phys. Rev. B **34**, 4350 (1986).

[7]A. L. Ageev, Yu. A. Babanov, N. V. Ershov, and V. V. Vasin, Phys. Status Solidi B **108**, 103 (1981).

[8]P. Eisenberger and G. S. Brown, Solid State Commun. **29**, 481 (1979).

[9]E. D. Crozier and A. J. Seary, Can. J. Phys. **58**, 1388 (1980).

[10]G. S. Cargill III, J. Non-Cryst. Solids **61**, 261 (1984).

[11]R. Frahm, R. Haensel, and P. Rabe, in *EXAFS and Near Edge Structure,* edited by A. Bianconi, L. Incoccia, and S. Stipcich (Springer-Verlag, Berlin, 1983), p. 107.

[12]J. Kortright, W. Warburton, and A. Bienenstock, in *EXAFS and Near Edge Structure* (Ref. 11), p. 362.

[13]M. L. Theye, A. Gheorghin, and H. Launois, J. Phys. C **13**, 6569 (1980).

[14]E. A. Stern, Y. Ma, and C. E. Bouldin, Phys. Rev. Lett. **57**, 1659 (1987).

[15]M. A. Marcus, Phys. Rev. Lett. **57**, 1658 (1987).

[16]P. A. Lee and J. B. Pendry, Phys. Rev. B **11**, 2795 (1975).

[17]P. J. Durham, J. B. Pendry, and C. H. Hodges, Comput. Phys. Commun. **25**, 193 (1982).

[18]S. J. Gurman, N. Binsted, and I. Ross, J. Phys. C **17**, 143 (1984).

[19]S. J. Gurman, J. Phys. C **21**, 3699 (1988).

[20]J. E. Harries, D. W. L. Hukins, and S. S. Hasnain, J. Phys. C **19**, 6859 (1986).

[21]F. W. Lytle, D. E. Sayers, and E. A. Stern, Physica B **158**, 710 (1989).

[22]C. E. Bouldin and E. A. Stern, in *EXAFS and Near Edge Structure III,* edited by K. O. Hodgson, B. Hedman, and J. E. Penner-Hahn (Springer-Verlag, Berlin, 1984), p. 273; E. A. Stern, in *Physics of Disordered Materials,* edited by H. Fritzche and S. R. Ovshinsky (Plenum, New York, 1985), p. 143; C. E. Bouldin, Ph.D. thesis, University of Washington, 1984 (unpublished).

[23]E. A. Stern, B. Bunker, and S. M. Heald, Phys. Rev. B **21**, 5521 (1980).

[24]E. A. Stern, P. Livins, and Z. Zhang, Phys. Rev. B **43**, 8850 (1991).

[25]J. J. Rehr (private communication).

[26]R. Kubo, J. Phys. Soc. Jpn. **17**, 1100 (1962).

[27]L. Brillouin, *Science and Information Theory,* 2nd ed. (Academic, New York, 1962).

[28]M. Cooper and K. Robinson, Acta Crystallogr. **20**, 614 (1966).

[29]Y. Ma and E. A. Stern, Phys. Rev. B **38**, 3754 (1988).

[30]A. D. I. Nicolo, Acta Crystallogr. **6**, 285 (1953).

[31]R. E. Stenkamp, L. C. Sieker, and L. H. Jensen, J. Am. Chem. Soc. **106**, 618 (1984); J. Inorg. Biochem. **19**, 247 (1983); Acta Crystallogr. B **38**, 784 (1982).

[32]W. T. Elam, E. A. Stern, J. D. McCallum, and J. Sanders-Loehr, J. Am. Chem. Soc. **104**, 6369 (1982).